Selective enrichment of hypericin in malignant glioma: Pioneering *in vivo* results

SUSAN NOELL[1], DANIEL MAYER[1], WOLFGANG S.L. STRAUSS[2], MARCOS S. TATAGIBA[1] and RAINER RITZ[1]

[1]Department of Neurosurgery, Eberhard Karls Universität Tübingen, Hoppe-Seyler-Str. 3, 72076 Tübingen;
[2]Institut für Lasertechnologien in der Medizin und Messtechnik an der Universität Ulm, Helmholtzstr. 12, 89081 Ulm, Germany

Received November 16, 2010; Accepted January 18, 2011

DOI: 10.3892/ijo.2011.968

Abstract. Malignant gliomas are diffuse infiltrative growing tumors with a poor prognosis despite treatment with a combination of surgery, radiotherapy and chemotherapy. It has been shown recently that complete tumor resection improves the survival time significantly. Hypericin, a component of St. Johns Wort, is one of the most powerful photosensitizers in nature. The aim of the present study was to investigate accumulation of hypericin in intracerebral implanted malignant glioma *in vivo*. Rats underwent stereotactic implantation of C6 glioma cells. After intravenous administration of hypericin (5 mg per kg body weight), accumulation of the compound was studied in tumor, the infiltration zone surrounding the tumor and healthy brain (contralateral hemisphere) by fluorescence microscopy between 0 and 48 h after injection. Results were compared by one-way analysis of variance. For *post hoc* pair-wise comparison the Tukey-Kramer HSD test was used. Accumulation of hypericin was significantly higher in C6 glioma as compared to normal tissue. Maximum hypericin uptake was achieved at 24 h after injection. Ratios of fluorescence intensity between tumor and normal tissue as well as infiltration zone and normal tissue of about 6.1:1 and 1.4:1 were found. Considering tissue auto-fluorescence, fluorescence ratios of about 19.8:1 and 2.5:1 were calculated, respectively. Therefore, hypericin seems to be quite an effective fluorescence marker for the detection of glioma *in vivo*. To the best of our knowledge, the present study demonstrates for the first time that hypericin accumulates selectively in intracerebral implanted C6 glioma *in vivo* after systemic (intravenous) administration.

Introduction

Patients who are suffering from glioblastoma represent the main proportion of patients with malignant brain tumors and show simultaneously the shortest survival time (1). Surgical therapy aims for a total resection of the tumor while preserving the surrounding normal brain tissue and thus the functional integrity of patients. Glioblastoma is an ill-defined, diffuse infiltrative growing tumor. Discrimination between tumor and normal brain tissue during surgery is elementary. A method to visualize residual tumor tissue will be a considerable advantage leading to safer and more complete tumor resection, because tumors relapse immediately at their margins of resection despite adjuvant therapy in approximately 90% of patients (2-10). Improvement of radicality in tumor resection by intraoperative visualization was demonstrated by Stummer *et al*. They used oral administration of 5-aminolevulinic acid (5-ALA), which is metabolized in the tumor cells to fluorescent protoporphyrin IX (PpIX). With this approach complete tumor resection was achieved in 65% of patients as compared to 36%, when tumor resection is performed under conventional white light conditions. This resulted in an extension of median survival time from 11.8 to 16.7 months in the fluorescence-guided resection group (11,12). Additionally, new therapeutic options, i.e., chemotherapy with the alkylating agent temozolomide and antiangiogenic drugs (e.g., bevacizumab), ensured further progress in glioma therapy (13-15). Despite enormous progress in the surgical and chemotherapeutical treatment of malignant brain tumors during the last decade, the prognosis of glioblastoma patients is still unfavourable. Photodynamic therapy (PDT) as an additional local treatment tool might be of interest in glioblastoma therapy in the future (16-19). PDT is an interesting modality of cancer treatment, which is based on the selective accumulation of a photosensitizer (PS) in tumor tissue. Illumination with light of appropriate wavelength produces reactive oxygen species (ROS), which react with biomolecules inducing mechanisms of apoptosis or necrosis and leading finally to cell death (20).

Hypericin, a constituent of St. Johns Wort (SJW; *Hypericum perforatum*), is one of the most powerful natural photosensitizers (21). *In vitro* and *in vivo* photodynamic effects inducing apoptosis and/or necrosis of various malignant cells, such as human glioblastoma cell lines (22), human HL-60 promyelocytic leukaemia cells and $CD4^+$ T-cells (23), rat bladder transitional cell carcinoma (24), human colon carcinoma and hepatoma cell lines (25) as well as human pancreatic cancer (26), were demonstrated. *In vitro* hypericin accumulates in glioma cells significantly higher than in neurones (27,28). However, hypericin could not be detected in healthy rat brain *in vivo* after oral administration of either alcoholic *H. perforatum* extracts or

Correspondence to: Dr Rainer Ritz, Department of Neurosurgery, University Hospital Tübingen, Hoppe-Seyler-Str. 3, 72076 Tübingen, Germany
E-mail: rainer_ritz@hotmail.com

Key words: hypericin, fluorescence diagnosis, malignant glioma, C6 glioma

the pure compound (29-31). These findings encouraged us to investigate accumulation of hypericin after systemic (intravenous) administration in C6 rat glioma, which is characterized by a disrupted blood-brain barrier (BBB). Particular interest was given to the relation between application time and hypericin enrichment in the tumor. Additionally, hypericin uptake in the tumor was compared to that in the infiltration zone around the tumor as well as in healthy brain of the contralateral hemisphere.

Materials and methods

Cell culture. Rat glioma C6 cells (ATCC Number CCL-107; American Type Culture Collection, Rockville, MD, USA) were grown in 75 cm^2 flasks (Corning, NY, USA) with RPMI medium containing 10% fetal bovine serum and penicillin (10,000 U/ml) as well as streptomycin (10,000 μg/ml) (Invitrogen, Karlsruhe, Germany). Cells were cultured for 3 days until confluence was achieved. After washing with phosphate buffered saline (PBS, Invitrogen) cells were detached, centrifugated and resuspended in PBS for implantation in rat brain.

In vivo implantation of cultivated C6 cells. The animals were treated in accordance to the guidelines of the University of Tübingen animal ethics committee and the German Animal Welfare Act. A total of 16 male Wistar rats purchased from Charles River (Sulzfeld, Germany) weighting 200-250 g underwent stereotactic implantation of glioma C6 cells (10^5) in a volume of 2 μl PBS. Rats were anaesthetized using a combination of fentanyl (0.005 mg/kg), midazolam (2.0 mg/kg) and medetomidine (0.15 mg/kg) body weight by intraperitoneal injection. A frontal, 10 mm sagittal scalp incision in the midline was performed. A burr hole was made 2 mm lateral to the sagittal suture and 2 mm in front of the coronar suture using a microsurgical drill. Rats were fixed in the stereotactic frame and the cell suspension was slowly inoculated intracerebrally at a depth of 2 mm. The burr hole was closed using bone wax and the scalp was sewed.

On day ten after tumor implantation the animals were anaesthetized as mentioned before. Hypericin [obtained from Phytochem, Ichenhausen, Germany, with a purity higher than 99% and dissolved in DMSO, PEG and aqua injectabile as described by van de Putte *et al* (32)] was administered at a dose of 5 mg/kg body weight via the lateral tail vein. Animals were sacrificed at 2, 6, 12, 24, 36 and 48 h after injection and the brain was withdrawn, covered in Tissue Tek (Invitrogen) and immediately frozen in liquid nitrogen. Rats bearing C6 glioma without photosensitization as well as healthy rats after hypericin administration served as controls.

Fluorescence microscopy. Coronal slices with a thickness of 7 μm were prepared with a cryomicrotome (Microm HM 560, Microm International GmbH, Walldorf, Germany). Slices for fluorescence microscopy were stained with DAPI Vectashield Mounting medium at a concentration of 1.5 μg/ml (Vector Labaratories, Burlingame, USA) and covered with antifade medium (Dako, Hamburg, Germany) on cover slips (Super Frost Plus, Langenbrinck Labor und Medizintechnik, Emmendingen, Germany). Corresponding serial slices were stained by hematoxylin and eosin (H&E) for histologic assessment.

Fluorescence microscopy was carried out using an Olympus BX61 microscope (Olympus-Europa GmbH, Hamburg, Germany) equipped with a UPlanFI 40x/0.75 objective and filter sets for the detection of red fluorescence (hypericin, U MWG2; excitation: 510-550 nm, emission: >590 nm) as well as blue fluorescence (DAPI, U MWU; Excitation 330-385 nm, emission: >420 nm). Fluorescence images were obtained using an F-View II charge-coupled device camera (Olympus Soft Imaging Solutions GmbH, Münster, Germany).

Each slice used for fluorescence microscopy was divided into three zones: tumor, infiltration zone and normal tissue, i.e., corresponding contralateral area usually 50-100 μm distant to the tumor border. In every zone 30 regions of interest (ROIs) were defined and fluorescence intensity was measured under identical conditions. Values of fluorescence intensity and autofluorescence, defined as the fluorescence measured with the U MWG2 filter in slices from healthy brain without hypericin administration, were given in arbitrary units. For each animal at least 12 slices were investigated. All procedures, i.e., preparation and storage of slices and fluorescence measurements, were performed under subdued light or in the dark.

Statistical analyses. Fluorescence intensities in the tumor, infiltration zone and normal brain were compared by one-way analysis of variance. For *post hoc* pair-wise comparison the Tukey-Kramer HSD test was used. Global significance level was $p<0.05$. Mean values and 95% confidence intervals are given. All statistical methods were carried out with the statistical software package, JMP version 8.0.2 (www.JMP.com).

Results

In order to determine the tumor selectivity of hypericin uptake coronar cryosections of rat brains were investigated. To identify tumor tissue histologically, H&E staining was performed for every second serial section. The subsequent serial sections were stained by DAPI and investigated by fluorescence microscopy using the appropriate filter settings to detect DAPI and hypericin fluorescence. As demonstrated in Fig. 1, hypericin accumulates selectively in C6 glioma, but not in normal rat brain tissue, after intravenous administration at a dose of 5 mg/kg body weight. Note the intensive red fluorescence of the C6 glioma due to hypericin accumulation. Additionally, the infiltration zone around the solid tumor shows also some hypericin uptake. This finding is shown in more detail in Fig. 2. Solid C6 glioma is characterized by a high density of cell nuclei (right side after H&E and DAPI staining) and the intense red fluorescence of hypericin. In contrast, no hypericin fluorescence is detected in the contralateral hemisphere without tumor (left side). Furthermore, hypericin fluorescence correlates well with the decreasing density of tumor cells in the infiltration zone of C6 glioma (middle).

As shown in Fig. 3, maximum of hypericin accumulation in C6 glioma is reached 24 h after intravenous administration. For longer time intervals, i.e., 36 and 48 h after injection, fluorescence intensity decreases rapidly. Mean values of hypericin fluorescence within tumor, infiltration zone and healthy brain tissue are summarized in Table I. There is significant higher fluorescence in tumor tissue as compared to normal tissue after administration of hypericin regardless to the time interval between injection

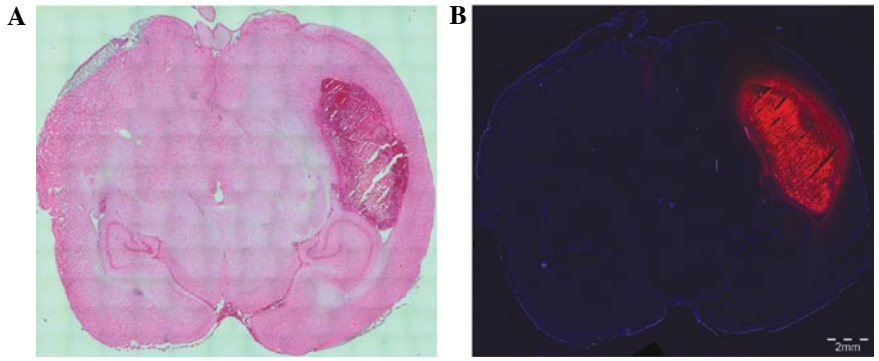

Figure 1. Overview of coronar cryosections of a rat brain after stereotactic implantation of C6 glioma. White-light microscopy after hematoxylin-eosin staining (A) and fluorescence microscopy after DAPI staining (B). Rats received 5 mg/kg body weight hypericin 24 h prior to preparation. Fluorescence microscopic images were visualized by U MWG2 filter (excitation, 510-550 nm; emission, >590 nm) for red fluorescence (hypericin) and U MWU filter (excitation, 330-385 nm; emission, >420 nm) for DAPI staining; magnification x4.

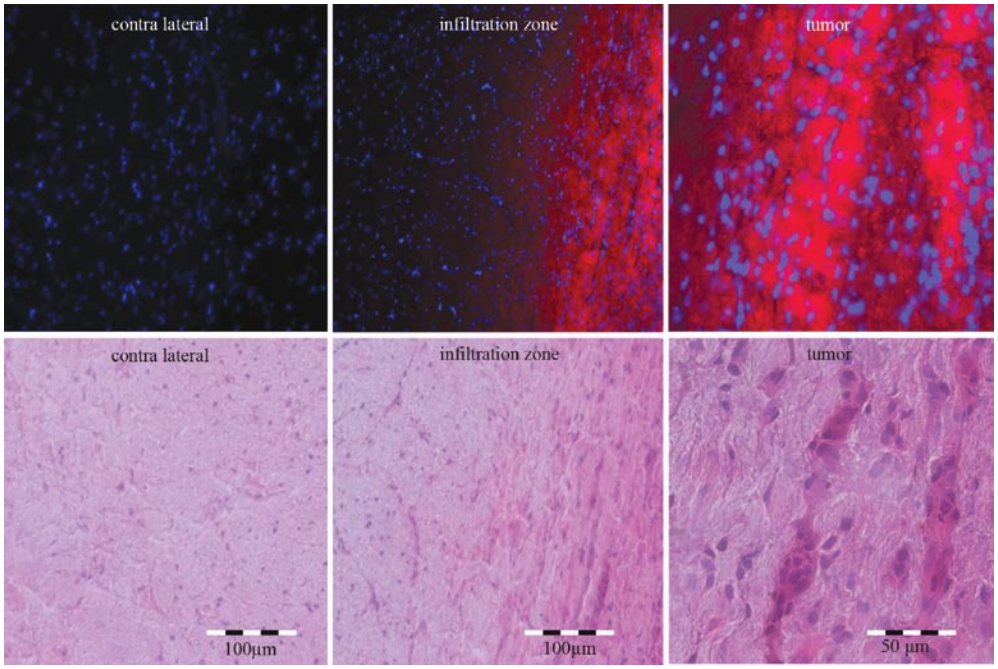

Figure 2. Cryosections of the C6 glioma in rat brain. Contralateral hemisphere without tumor (left), tumor infiltration zone (middle) and tumor (right). Selective hypericin accumulation (red fluorescence) in the tumor and tumor infiltration zone co-stained with DAPI (blue) is demonstrated in the upper row. Corresponding sections stained by hematotoxylin and eosin (lower row). Filter sets, see Fig. 1; magnification x20.

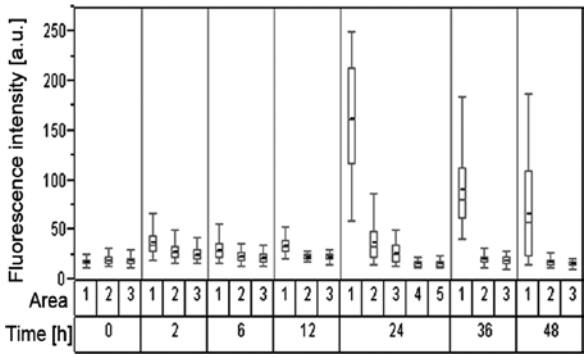

Figure 3. Mean fluorescence intensities and confidence intervals after intravenous injection of hypericin (5 mg/kg b.w.) at different times after administration (1-3) and controls (4-5); localizations: (1) tumor (2) infiltration zone (3) contralateral hemisphere (4) no tumor, left hemisphere and (5) no tumor, right hemisphere after PBS injection.

and brain removal. Additionally, the infiltration zone exhibits about 1.5-fold higher hypericin fluorescence as the contralateral hemisphere at 24 h after administration. Control experiments were performed in rats after stereotactic injection of PBS. Fluorescence intensity after PBS injection (16.2 a.u., area 5, Fig. 3) was quite similar to that of normal brain (16.0 a.u., area 4, Fig. 3).

Ratios of fluorescence intensity between tumor and normal tissue as well as infiltration zone and normal tissue of about 6.1:1 and 1.4:1 were found at 24 h after hypericin administration; considering tissue autofluorescence (Table I at 0 h) the ratios of about 19.8:1 and 2.5:1 were calculated, respectively. It should be mentioned, that the autofluorescence values of C6 glioma (19 a.u.), infiltration zone (20.25 a.u.) and normal brain tissue (19.6 a.u.) are quite similar.

Table I. Fluorescence intensities of different zones in C6 glioma bearing rat brains after i.v. administration of hypericin (5 mg/kg b.w.).

	Fluorescence intensity (a.u.) (95% confidence interval)			Tukey-Kramer HSD test (significance level: $p<0.05$)		
Time (h)	Tumor (T)	Infiltration zone (IZ)	Healthy brain (HB)	T vs HB	T vs IZ	IZ vs HB
0	19.0 (18.7-19.3)	20.25 (19.9-20.6)	19.60 (19.3-19.9)	0.0180	$<10^{-4}$	0.0096
2	38.34 (37.3-39.4)	28.93 (28.3-29.6)	26.30 (25.8-26.8)	$<10^{-5}$	$<10^{-5}$	$<10^{-4}$
6	30.55 (29.8-31.3)	23.85 (23.4-24.3)	22.67 (22.2-23.2)	$<10^{-4}$	$<10^{-4}$	0.0168
12	35.85 (34.9-36.8)	23.08 (22.7-23.5)	23.05 (22.6-23.5)	$<10^{-4}$	$<10^{-4}$	*0.9973*
24	163.27 (159.4-167.2)	38.58 (37.0-40.1)	26.89 (26.2-27.6)	$<10^{-5}$	$<10^{-5}$	$<10^{-5}$
36	91.05 (88.2-93.9)	20.86 (20.5-21.2)	19.86 (19.5-20.2)	$<10^{-5}$	$<10^{-5}$	*0.7734*
48	67.65 (64.1-71.2)	18.37 (18.0-18.7)	16.12 (15.9-16.3)	$<10^{-5}$	$<10^{-5}$	*0.2820*

Mean fluorescence intensity and the 95% confidence interval (CI) in parentheses are given. Tukey-Kramer HSD test was applied to test the significance of fluorescence intensity according to localization. Significance level was $p<0.05$. Non-significant p-values are given in italic numbers.

Discussion

Hypericin is a component of SJW, also known as *H. perforatum*. SJW, a herbal medication, used over 2,000 years for various complaints, such as bronchitis, inflammation of the throat or gastrointestinal tract disorders. Extracts of SJW contain a complex mixture of more than 150 components, including phloroglucinols such as hyperforin, naphtodianthrones such as hypericin and pseudohypericin, flavonoids such as quercetin, quercitrin and rutin, as well as other constituents (33).

SJW extracts are well established in the therapy of mild to moderate depression and are of equal efficiency compared to tricyclic antidepressants, monoamine oxidase (MAO) inhibitors and selective serotonine reuptake inhibitors. The relevance of hypericin regarding the antidepressive effect is controversially discussed. However, inhibitory effects of MAO enzymes could not be confirmed. In order to gain more clarity Paulke *et al* developed a new method for the detection of hypericin using a HPLC method. After oral administration of either SJW extracts or pure hypericin the authors could not find any hypericin in the brains of healthy rats (29,31). Gaccia and Gobbi confirmed this result in 2009 (30). Fox *et al* investigated the pharmocokinetics of hypericin in plasma and cerebrospinal fluid in non-human primates (34). Notably, the compound was not detected in the cerebrospinal fluid after intravenous administration of pure hypericin (2 and 5 mg/kg body weight).

This findings are probably due to an intact blood-brain barrier (BBB), separating extracellular fluid in the brain from blood circulation. The BBB is formed by the endothelial cells of brain microvessels, which are connected by specialized tight junctions. These microvessels are surrounded by pericytes and astrocytic endfeets, building the so-called glio-vascular complex. Only lipophilic and small molecules with a molecular weight of less than 400 g/mol can cross the BBB via free diffusion (35). All other molecules need specific BBB transport systems, classified in a) carrier-mediated transporters (CMT), b) active efflux transporters (AET) and c) receptor-mediated transporters (RMT). The present data strongly indicate, that penetration of the highly lipophilic hypericin (molecular weight of 504 g/mol), across an intact BBB is very low. Thus, quite selective hypericin accumulation in intracerebrally implanted C6 gliomas in Wistar rats as demonstrated in Fig. 1 is likely to be due to an impairment of the BBB in the tumor.

In the present investigation, maximum hypericin accumulation in intracerebrally implanted C6 glioma was achieved at 24 h after intravenous administration. However, other *in vivo* investigations using different subcutaneously implanted tumor cell lines in mice found maximum hypericin accumulation at 4-6 h after intravenous injection (32,36,37). In addition, maximum hypericin accumulation in subcutaneously implanted prostate cancer cells (LNCaP) was found at 1-2 h after oral administration of 5 mg/kg hypericin (38). Tissue distribution of hypericin was studied in Fischer rats bearing subcutaneously inoculated AY-27 cells (rat bladder transitional cell carcinoma) after intravenous administration (1 and 5 mg/kg body weight). The highest concentrations of hypericin were determined in plasma as well as in liver, spleen and lung tissue. Again negligible amounts of hypericin were found in brain tissue (39). Also other fluorescence markers were investigated in *in vivo* rat glioma models. Kabuto *et al* detected the maximum of fluorescein fluorescence at 1 h after intravenous administration in a C6 rat glioma model (40).

Madsen *et al* studied 5-ALA-derived PpIX fluorescence in tumor, normal brain and by the authors the so called brain-adjacent-to-tumor (BAT) zone after stereotactic implantation of BT4C tumor cells in BD-IX inbred rats (41). PpIX distribution was determined at 4-5 h after intraperitoneal injection of 60 mg/kg 5-ALA. In normal brain tissue fluorescence intensity was less than 1% as compared to tumor fluorescence; in the BAT zone it was up to 20% of the fluorescence intensity of tumor tissue. Angell-Petersen *et al* compared the biodistribution of PpIX between tumor and contralateral brain by fluorescence measurements 4-5 h after intraperitoneal injection of 60, 125 and 250 mg/kg 5-ALA. The authors found a selectivity ratio of at least 230:1 comparing tumor to normal brain tissue (42). Stummer *et al* detected maximum of 5-ALA-derived PpIX fluorescence in

the C6 rat glioma model at 6 h after intravenous administration of 100 mg/kg body weight 5-ALA and a fluorescence ratio between tumor and normal tissue of 6:1 was determined (43).

In the present study maximum accumulation of hypericin in C6 glioma was found at 24 h after intravenous administration. Although the time interval between administration and maximum accumulation in tumor tissue is significantly longer in the case of hypericin as compared to 5-ALA-derived PpIX, the tissue selectivity of both photosensitizers seem to be quite similar (as deduced from the fluorescence ratios between tumor and normal tissue). Experimental studies concerning the first generation of PS, namely haematoporphyrin derivative (HDP), a mixture of different porphyrins, revealed a accumulation ratio of up to 12:1 of PS in the tumor as compared to normal brain (44,45). For meta-tetrahydroxyphenylchlorin (mTHPC), a second generation PS, a ratio of more than 80:1 has been described *in vivo* (implantation of C6 glioma in Spraque-Dawley rats) (46).

In conclusion, to the best of our knowledge the present study demonstrates for the first time that hypericin accumulates selectively in C6 glioma *in vivo* after systemic (intravenous) administration. Therefore, hypericin seems to be quite an effective fluorescence marker for the detection of glioma *in vivo*. Since this compound exhibits excellent photosensitizing properties, it might also be of advantage in glioma therapy. Further *in vivo* investigations should be initiated to prove this hypothesis.

Acknowledgements

Technical assistance by A. Gruber, Department of Neurosurgery, Eberhard Karls Universität, is gratefully acknowledged.

References

1. Ohgaki H: Epidemiology of brain tumors. Methods Mol Biol 472: 323-342, 2009.
2. Ammirati M, Vick N, Liao YL, Ciric I and Mikhael M: Effect of the extent of surgical resection on survival and quality of life in patients with supratentorial glioblastomas and anaplastic astrocytomas. Neurosurgery 21: 201-206, 1987.
3. Barker FG, Chang SM, Larson DA, Sneed PK, Wara WM, Wilson CB and Prados MD: Age and radiation response in glioblastoma multiforme. Neurosurgery 49: 1288-1297, 2001.
4. Bashir R, Hochberg F and Oot R: Regrowth patterns of glioblastoma multiforme related to planning of interstitial brachytherapy radiation fields. Neurosurgery 23: 27-30, 1988.
5. Brandes AA, Tosoni A, Franceschi E, *et al*: Recurrence pattern after temozolomide concomitant with and adjuvant to radiotherapy in newly diagnosed patients with glioblastoma: correlation with MGMT promoter methylation status. J Clin Oncol 27: 1275-1279, 2009.
6. Buckner JC: Factors influencing survival in high-grade gliomas. Semin Oncol 30: 10-14, 2003.
7. Davis FG, Freels S, Grutsch J, Barlas S and Brem S: Survival rates in patients with primary malignant brain tumors stratified by patient age and tumor histological type: an analysis based on Surveillance, Epidemiology, and End Results (SEER) data, 1973-1991. J Neurosurg 88: 1-10, 1998.
8. Ekinci G, Akpinar IN, Baltacioglu F, Erzen C, Kilic T, Elmaci I and Pamir N: Early-postoperative magnetic resonance imaging in glial tumors: prediction of tumor regrowth and recurrence. Eur J Radiol 45: 99-107, 2003.
9. Lacroix M, Abi-Said D, Fourney DR, *et al*: A multivariate analysis of 416 patients with glioblastoma multiforme: prognosis, extent of resection, and survival. J Neurosurg 95: 190-198, 2001.
10. McGirt MJ, Chaichana KL, Gathinji M, *et al*: Independent association of extent of resection with survival in patients with malignant brain astrocytoma. J Neurosurg 110: 156-162, 2009.
11. Stummer W, Pichlmeier U, Meinel T, Wiestler OD, Zanella F and Reulen HJ: Fluorescence-guided surgery with 5-aminolevulinic acid for resection of malignant glioma: a randomised controlled multicentre phase III trial. Lancet Oncol 7: 392-401, 2006.
12. Stummer W, Reulen HJ, Meinel T, *et al*: Extent of resection and survival in glioblastoma multiforme: identification of and adjustment for bias. Neurosurgery 62: 564-576, 2008.
13. Stupp R, Hegi ME, Mason WP, *et al*: Effects of radiotherapy with concomitant and adjuvant temozolomide versus radiotherapy alone on survival in glioblastoma in a randomised phase III study: 5-year analysis of the EORTC-NCIC trial. Lancet Oncol 10: 459-466, 2009.
14. Stupp R, Mason WP, van den Bent MJ, *et al*: Radiotherapy plus concomitant and adjuvant temozolomide for glioblastoma. N Engl J Med 352: 987-996, 2005.
15. Van Meir EG, Hadjipanayis CG, Norden AD, Shu HK, Wen PY and Olson JJ: Exciting new advances in neuro-oncology: the avenue to a cure for malignant glioma. CA Cancer J Clin 60: 166-193, 2010.
16. Eljamel MS, Goodman C and Moseley H: ALA and Photofrin fluorescence-guided resection and repetitive PDT in glioblastoma multiforme: a single centre Phase III randomised controlled trial. Lasers Med Sci 23: 361-367, 2008.
17. Stepp H, Beck T, Pongratz T, Meinel T, Kreth FW, Tonn JC and Stummer W: ALA and malignant glioma: fluorescence-guided resection and photodynamic treatment. J Environ Pathol Toxicol Oncol 26: 157-164, 2007.
18. Stylli SS, Kaye AH, MacGregor L, Howes M and Rajendra P: Photodynamic therapy of high grade glioma - long term survival. J Clin Neurosci 12: 389-398, 2005.
19. Stylli SS and Kaye AH: Photodynamic therapy of cerebral glioma - a review. Part II - clinical studies. J Clin Neurosci 13: 709-717, 2006.
20. Dougherty TJ, Gomer CJ, Henderson BW, *et al*: Photodynamic therapy. J Natl Cancer Inst 90: 889-905, 1998.
21. Vandenbogaerde AL, Kamuhabwa A, Delaey E, Himpens BE, Merlevede WJ and De Witte PA: Photocytotoxic effect of pseudohypericin versus hypericin. J Photochem Photobiol B 45: 87-94, 1998.
22. Miccoli L, Beurdeley-Thomas A, De Pinieux G, Sureau F, Oudard S, Dutrillaux B and Poupon MF: Light-induced photoactivation of hypericin affects the energy metabolism of human glioma cells by inhibiting hexokinase bound to mitochondria. Cancer Res 58: 5777-5786, 1998.
23. Lavie G, Kaplinsky C, Toren A, Aizman I, Meruelo D, Mazur Y and Mandel M: A photodynamic pathway to apoptosis and necrosis induced by dimethyl tetrahydroxyhelianthrone and hypericin in leukaemic cells: possible relevance to photodynamic therapy. Br J Cancer 79: 423-432, 1999.
24. Kamuhabwa AA, Cosserat-Gerardin I, Didelon J, *et al*: Biodistribution of hypericin in orthotopic transitional cell carcinoma bladder tumors: implication for whole bladder wall photodynamic therapy. Int J Cancer 97: 253-260, 2002.
25. Couladis M, Badisa RB, Baziou P, Chaudhuri SK, Pilarinou E, Verykokidou E and Harvala C: Antioxidant and cytotoxic activities of Hypericum sp. on brine shrimps and human cancer cell lines. Phytother Res 16: 719-722, 2002.
26. Liu CD, Kwan D, Saxton RE and McFadden DW: Hypericin and photodynamic therapy decreases human pancreatic cancer *in vitro* and *in vivo*. J Surg Res 93: 137-143, 2000.
27. Ritz R, Muller M, Weller M, Dietz K, Kuci S, Roser F and Tatagiba M: Hypericin: a promising fluorescence marker for differentiating between glioblastoma and neurons *in vitro*. Int J Oncol 27: 1543-1549, 2005.
28. Uzdensky AB, Bragin DE, Kolosov MS, Kubin A, Loew HG and Moan J: Photodynamic effect of hypericin and a water-soluble derivative on isolated crayfish neuron and surrounding glial cells. J Photochem Photobiol B 72: 27-33, 2003.
29. Wurglics M and Schubert-Zsilavecz M: Hypericum perforatum: a 'modern' herbal antidepressant: pharmacokinetics of active ingredients. Clin Pharmacokinet 45: 449-468, 2006.
30. Caccia S and Gobbi M: St. John's wort components and the brain: uptake, concentrations reached and the mechanisms underlying pharmacological effects. Curr Drug Metab 10: 1055-1065, 2009.
31. Paulke A, Schubert-Zsilavecz M and Wurglics M: Determination of hypericin and pseudohypericin from Hypericum perforatum in rat brain after oral administration. Monatsh Chem 139: 489-494, 2008.
32. Van De Putte M, Roskams T, Bormans G, Verbruggen A and De Witte PA: The impact of aggregation on the biodistribution of hypericin. Int J Oncol 28: 655-660, 2006.

33. Saller R, Melzer J and Reichling J: [St. John's Wort (Hypericum perforatum): a plurivalent raw material for traditional and modern therapies]. Forsch Komplementarmed Klass Naturheilkd 10 (Suppl 1): 33-40, 2003.
34. Fox E, Murphy RF, McCully CL and Adamson PC: Plasma pharmacokinetics and cerebrospinal fluid penetration of hypericin in nonhuman primates. Cancer Chemother Pharmacol 47: 41-44, 2001.
35. Pardridge WM: Molecular biology of the blood-brain barrier. Mol Biotechnol 30: 57-70, 2005.
36. Chung PS, Saxton RE, Paiva MB, *et al*: Hypericin uptake in rabbits and nude mice transplanted with human squamous cell carcinomas: study of a new sensitizer for laser phototherapy. Laryngoscope 104: 1471-1476, 1994.
37. Du HY, Bay BH and Olivo M: Biodistribution and photodynamic therapy with hypericin in a human NPC murine tumor model. Int J Oncol 22: 1019-1024, 2003.
38. Xie X, Hudson JB and Guns ES: Tumor-specific and photo-dependent cytotoxicity of hypericin in the human LNCaP prostate tumor model. Photochem Photobiol 74: 221-225, 2001.
39. Zupko I, Kamuhabwa AR, D'Hallewin MA, Baert L and De Witte PA: *In vivo* photodynamic activity of hypericin in transitional cell carcinoma bladder tumors. Int J Oncol 18: 1099-1105, 2001.
40. Kabuto M, Kubota T, Kobayashi H, *et al*: Experimental and clinical study of detection of glioma at surgery using fluorescent imaging by a surgical microscope after fluorescein administration. Neurol Res 19: 9-16, 1997.
41. Madsen SJ, Angell-Petersen E, Spetalen S, Carper SW, Ziegler SA and Hirschberg H: Photodynamic therapy of newly implanted glioma cells in the rat brain. Lasers Surg Med 38: 540-548, 2006.
42. Angell-Petersen E, Spetalen S, Madsen SJ, *et al*: Influence of light fluence rate on the effects of photodynamic therapy in an orthotopic rat glioma model. J Neurosurg 104: 109-117, 2006.
43. Stummer W, Stocker S, Novotny A, *et al*: *In vitro* and *in vivo* porphyrin accumulation by C6 glioma cells after exposure to 5-aminolevulinic acid. J Photochem Photobiol B 45: 160-169, 1998.
44. Kostron H: Photodynamische Therapie in der Neurochirurgie. In: Klinische Fluoreszenzdiagnostik Und Photodynamische Therapie. 1st edition. Szeimies RM, Jocham D and Landthaler M (eds). Blackwell Verlag GmbH, Berlin, pp299-322, 2003.
45. Kaye AH and Hill JS: Photodynamic therapy of brain tumours. Ann Acad Med Singapore 22: 470-481, 1993.
46. Obwegeser A, Jakober R and Kostron H: Uptake and kinetics of 14C-labelled meta-tetrahydroxyphenyl chlorin and 5-aminolaevulinic acid in the C6 rat glioma model. Br J Cancer 78: 733-738, 1998.